AD-A150 094 EXPLORATION OF NEW METHODS TO PRODUCE EFFICIENT SOURCES 1/1
OF COHERENT NEAR..(U) MASSACHUSETTS INST OF TECH
CAMBRIDGE GEORGE R HARRISON SPECTR.. M S FELD ET AL.
UNCLASSIFIED 16 NOV 84 ARO-19608.1-PH DAAG29-83-K-0017 F/G 17/5 NL

END
FILMED
DTIC

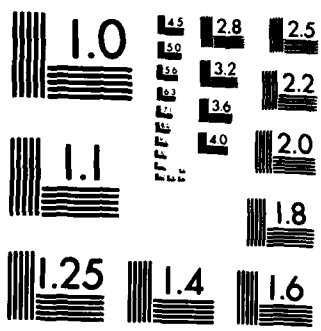

(2)

UNCLASSIFIED
SECURITY CLASSIFICATION OF THIS PAGE (When Data Entered)

REPORT DOCUMENTATION PAGE		READ INSTRUCTIONS BEFORE COMPLETING FORM
1. REPORT NUMBER: ARO 19608.1-PH	2. GOVT ACCESSION NO.: AD-A150 094 N/A	3. RECIPIENT'S CATALOG NUMBER: N/A
4. TITLE (and Subtitle): Exploration of New Methods to Produce Efficient Sources of Coherent Near Millimeter Wave Radiation		5. TYPE OF REPORT & PERIOD COVERED: Final, Nov. 1982 - May 1984
		6. PERFORMING ORG. REPORT NUMBER
7. AUTHOR(s): Michael S. Feld, R. R. Dasari, John E. Thomas		8. CONTRACT OR GRANT NUMBER(s): DAAG 29-83-K-0017
9. PERFORMING ORGANIZATION NAME AND ADDRESS: George R. Harrison Spectroscopy Laboratory, Massachusetts Institute of Technology, Rm 6-014 Cambridge, MA 02139		10. PROGRAM ELEMENT, PROJECT, TASK AREA & WORK UNIT NUMBERS
11. CONTROLLING OFFICE NAME AND ADDRESS: U. S. Army Research Office, Post Office Box 12211, Research Triangle Park, NC 27709		12. REPORT DATE: Nov. 16, 1984
		13. NUMBER OF PAGES: 17
14. MONITORING AGENCY NAME & ADDRESS(if different from Controlling Office)		15. SECURITY CLASS. (of this report): Unclassified
		15a. DECLASSIFICATION/DOWNGRADING SCHEDULE

16. DISTRIBUTION STATEMENT (of this Report)

Approved for public release; distribution unlimited.

17. DISTRIBUTION STATEMENT (of the abstract entered in Block 20, if different from Report)

NA

18. SUPPLEMENTARY NOTES

The view, opinions, and/or findings contained in this report are those of the author(s) and should not be construed as an official Department of the Army position, policy, or decision, unless so designated by other documentation.

19. KEY WORDS (Continue on reverse side if necessary and identify by block number)

Infrared, Near Millimeter Waves, Lasers, Photon Recyclers.

20. ABSTRACT (Continue on reverse side if necessary and identify by block number)

A summary is presented of a feasibility study for a new concept "photon recycling" which was proposed as a new means of generating near millimeter wave radiation using gas dynamic cooling. A general theoretical analysis of this concept is presented which shows that small partition fractions and low temperatures lead to an unwieldly geometry for the nozzle design.

DD FORM 1 JAN 73 1473 EDITION OF 1 NOV 65 IS OBSOLETE

UNCLASSIFIED

"Exploration of New Methods to Produce Efficient Sources of Coherent Near Millimeter Wave Radiation"

FINAL REPORT

For the Period November 1982 - May 1984

Michael S. Feld

John E. Thomas

Ramachandra R. Dasari

U.S. ARMY RESEARCH OFFICE

Grant No. DAAG29-83-K-0017

Massachusetts Institute of Technology

77 Massachusetts Avenue

Cambridge, MA 02139

Introduction

We have undertaken an investigation of new methods to produce efficient sources of coherent near millimeter wave (NMMW) radiation. A new concept, "photon recyling", was proposed as a possible means of achieving this goal. The photon recycler is basically a heat engine in which heat and infrared energy are absorbed in a hot region and NMMW power is emitted in a cold region, accompanied by expelled heat and the original infrared energy. The infrared photons play the role of a catalyst for the conversion of heat into NMMW power. In order to achieve cooling, a flowing system is employed in which molecules pass from a hot region through a nozzle and cool by adiabatic expansion.

Our approach to this problem has been two fold: (I) to obtain a detailed theoretical analysis of the gas dynamic photon recycling; and (II) to study experimentally the energy storage and flow in some candidate molecules.

Achieving photon recycling in practice has proven to be a difficult task. In order to clarify the situation, we have developed a simple and general analysis of gas dynamic photon recyclers which elucidates a number of important features and extends the results of our original proposal. This analysis (see Sec. I below) determines the requirements for optimum NMMW output. The primary difficulties arise from small partition fractions and low temperatures. The new analysis shows that this results in constraints on the nozzle in order to achieve infrared saturation in the cold region, and leads to an unwieldy geometry in which the nozzle must be very wide and thin, a rather impractical configuration.

In addition to carefully analyzing the photon recycling concept, a number of experiments (see Sec. II) have been undertaken to study the associated problem of infrared energy storage and collisional transfer in molecules, which is important for developing practical photon recycler systems. This has led to the development of a general time resolved IR-IR double resonance spectrometer which has been applied to study depolarizing and J transfer rates as well as K exchange rates.

Most recently, a new time resolved-velocity resolved grating technique has been developed with this system, which we believe will make it possible for the first time to obtain directly the velocity changing collision kernels for J-preserving and J transfer collisions. The technique permits kernels to be determined from the data without assumption about the kernel shape, and permits resolution of both classical and diffractive velocity changes. These important spin-offs will provide powerful new means for studying molecular scattering and energy transfer processes.

I. Analysis of Photon Recycling

The purpose of this section is to elucidate in a general way the conditions for obtaining maximum NMMW output for a given infrared (IR) amplifier, based on the IR photon recycling concept. This new analysis, based on the theoretical results presented in our proposal ("Exploration of New Methods to Produce Efficient Sources of Coherent Near Millimeter Wave Radiation", Aug. 1982) provides a general picture of photon recycling and clarifies a number of subtle features which initially were unappreciated.

Figure 1 is a schematic of a photon recycling system. It consists of an infrared amplifier A, a lumped infrared total loss L (due to all optics including photon recycler optics) and an ideal photon recycler (PR).

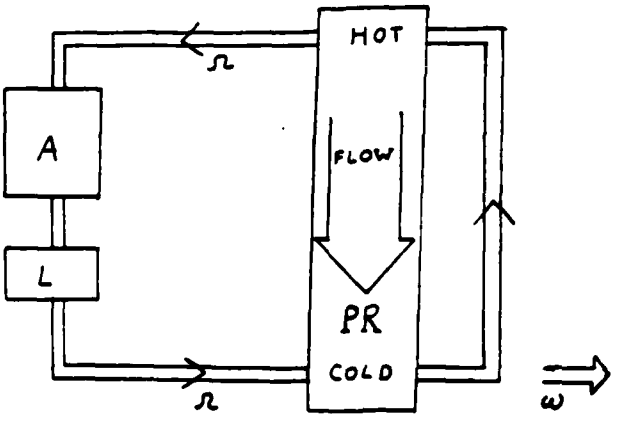

Fig. 1. Photon Recycling System

The recycler absorbs infrared power, ΔP_a, in the hot region and re-emits infrared power, ΔP_e, in the cold region. Assuming that gas dynamic expansion is used to achieve cooling, NMMW power is extracted at the cold low pressure side, so that rotational equilibration does not quench the NMMW population inversion. For this scheme, the energy level diagram is shown in Figure 2.

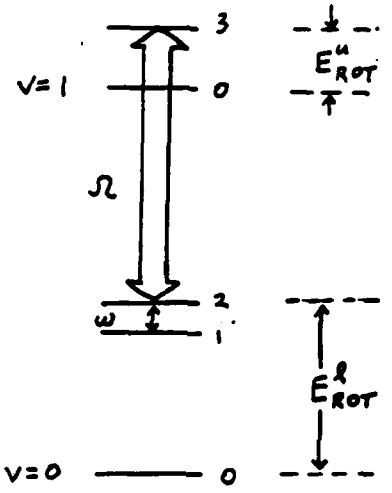

Fig. 2. Energy Level Diagram

The recycler works by absorbing IR photons, of frequency Ω, in the hot region on the 2 → 3 transition and then achieves a population inversion on the 3 → 2 transition by cooling. This requires that the upper level vibrational lifetime $1/\Gamma$ be longer than the molecule transit time through the whole system, and that the rotational energy E^u_{rot} be lower than E^l_{rot}. In the cold region, infrared photons stimulate emission on the 3 → 2 transition, creating an inversion on the 2 → 1 transition and hence NMMW gain at frequency ω.

A. Optimizing Amplifier Efficiency

Optimizing NMMW output requires that the amplifier be utilized at maximum efficiency. In general, this depends on two types of losses in the cavity. The first is the lumped loss L, which results in loss proportional to the cavity intensity. The second is the photon recycler net absorption loss, $\Delta P_a - \Delta P_e$, due to loss of stored infrared energy. An important and subtle point is that this second loss saturates at high cavity intensity and therefore cannot limit the cavity intensity. To optimize NMMW output, the maximum power, P_o, available from the given amplifier-loss (L) combination (peak of dashed curve of Fig. 3), must be expended in the photon recycler absorption loss,

$$P_o = \Delta P_a - \Delta P_e \tag{1}$$

Since the absorbed and emitted infrared powers are proportional to the flow $\dot{N}$ (molecules/sec), Eq.(1) determines the optimum flow and hence maximum NMMW output, provided that the IR and NMMW transitions are saturated (see below).

P_o is determined by maximizing the available infrared power by optimally balancing loss and saturation.

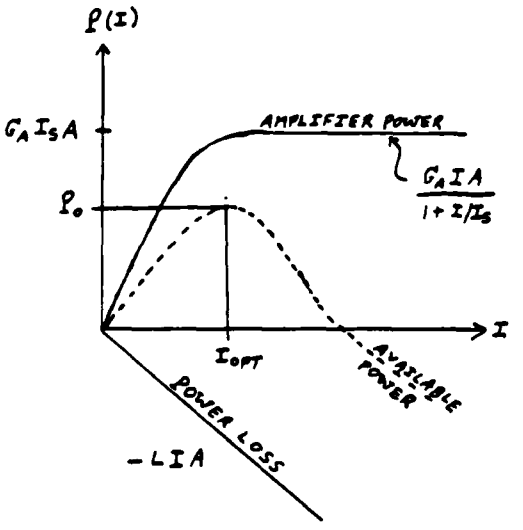

Fig. 3. Available infrared power versus intensity. I is varied by adjusting the flow, N.

As shown in Figure 3 (assuming homogeneous gain saturation), this occurs for $I = I_{opt}$, where

$$I_{opt} = I_s \left(\sqrt{\frac{G_A}{L}} - 1\right) \tag{2}$$

and

$$P_o = P(I_{opt}) = G_A I_S A \left(1 - \sqrt{\frac{L}{G_A}}\right)^2 \tag{3}$$

The amplifier area A, Gain , G_A, saturation intensity, I_S, and cavity loss, L, determine the maximum available power P_o which can be expended in the photon recycler. Equation (3) is just the optimum infrared power which would be transmitted out of the laser cavity if the PR were replaced with a beam splitter with optimum transmission. Since the gain is proportional to the amplifier length, P_o is a measure of the amplifier size. For a 1 meter CO_2 amplifier of area $A = 0.3\ cm^2$, reasonable parameters are listed in Table 1.

Table 1. CO_2 Amplifier/Loss Parameters

G_A	1.2 (1 m long amplifier)
I_S	55 W/cm^2*
A	0.3 cm^2
P_o	10W @ L = 10%

* L.E. Freed, C. Freed, and R.G. O'Donnell, IEEE J.Quan.El. QE-18, 1229 (1982).

The absorbed and emitted powers can be related to the flow $\dot{N}$ crossing the infrared laser beams. Assuming complete infrared saturation (see below),

$$\Delta P_a = \alpha_o \dot{N} \hbar\Omega \tag{4}$$

$$\Delta P_e = (\alpha_o - \alpha_e) \dot{N} \hbar\Omega \tag{5}$$

where, for moderately large rotational quantum numbers,

$$\alpha \simeq 1/(1+\exp(\Delta E/KT)) \tag{6}$$

is the fraction of molecules in the excited vibrational state for complete steady-state infrared saturation, and $\Delta E = \Delta E^{\ell}_{ROT} - \Delta E^{u}_{ROT} > 0$. The subscripts o and e refer to hot and cold regions of the PR, respectively. Figure 4 shows a plot of 2α versus $\Delta E/KT$.

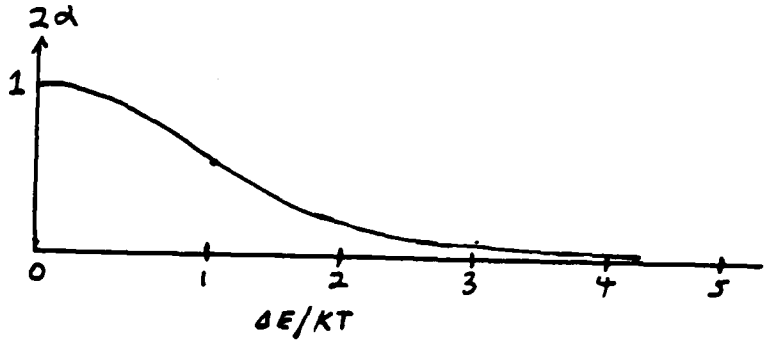

Fig. 4. Excited State Fraction.

Hot and cold temperatures must be chosen to yield a reasonable loss fraction, $\mathcal{L}$, of absorbed infrared power, given by

$$\mathcal{L} = \frac{\Delta P_a - \Delta P_e}{\Delta P_a} = \alpha_e/\alpha_o \tag{7}$$

For the present, $\mathcal{L}$ will be left unspecified. The optimum flow $\dot{N}$, is given in terms of α_o, P_o, and $\mathcal{L}$ as, (using Eq. (1)),

$$\dot{N} = P_o/(\mathcal{L}\alpha_o \hbar\Omega) \tag{8}$$

This choice extracts the maximum power for a given amplifier-loss combination.

B. NMMW Output

The NMMW small signal gain and saturation intensity can be estimated using a rate equation analysis based on Fig. 5.

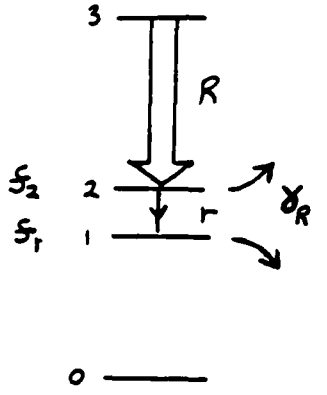

$R = \frac{\sigma_\Omega I_\Omega}{\hbar\Omega}$ Infrared transition rate.

$r = \frac{\sigma_\omega I_\omega}{\hbar\omega}$ NMMW transition rate.

γ_R Rotational equilibration rate.

Fig. 5. Rate Diagram

Neglecting the small difference in the level 1 and 2 population fractions (f_1 and f_2) yields

$$n_2 - n_1 = \frac{R}{\gamma_R + 2r}\,(n_3 - n_2) \tag{9}$$

valid for $\gamma_R(f_1 - f_2) \ll f_2 R$, where R, r are stimulated emission rates (Fig. 5). The population difference n_3-n_2 can be written as

$$n_3 - n_2 = \frac{1}{\sigma_\Omega I_\Omega}\frac{\partial I_\Omega(x,y)}{\partial x} = \frac{1}{R\hbar\Omega}\frac{\partial I_\Omega(x,y)}{\partial x}\,, \tag{10}$$

where the flow geometry is that of Fig. 6.

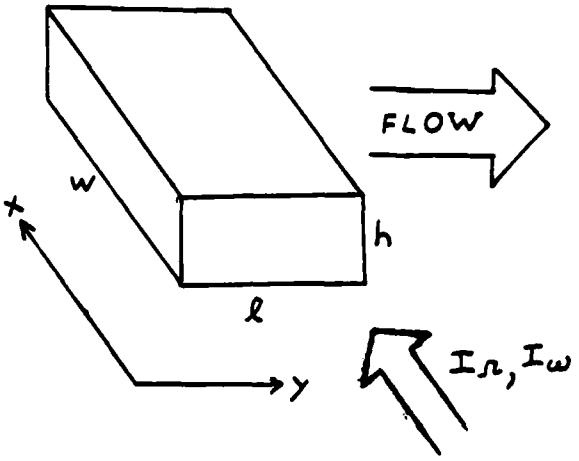

Fig. 6. Flow Geometry

The small signal NMMW gain ($r \rightarrow 0$) integrated along the propagation direction, x, and averaged over the flow direction y, is then

$$\bar{G}_\omega = \frac{1}{\ell}\int_0^\ell dy \int_0^w dx\, \sigma_\omega (n_2 - n_1)(x,y) = \frac{\sigma_\omega}{\gamma_R h \ell}\,\frac{\Delta P_e}{\hbar\Omega} \tag{11}$$

where the power emitted, ΔP_e, is given by Eq. 5. Using Eq. (1) and (7) gives

$$\bar{G}_\omega = \frac{\sigma_\omega P_o}{\hbar\Omega\gamma_R}\,\frac{1-\mathcal{L}}{\mathcal{L}}\,\frac{1}{h\ell} \tag{12}$$

The saturation intensity, defined by $2r/\gamma_R = I/I_\omega^{sat}$ at any point (x,y) is just

$$I_\omega^{SAT} = \frac{\hbar\omega\,\gamma_R}{2\,\sigma_\omega} \tag{13}$$

For large NMMW saturation everywhere, the maximum NMMW power will be determined in the same way as Eq. (3), with $L \rightarrow L_\omega$, $G_A \rightarrow \bar{G}_\omega$, and the area $A \rightarrow h\ell$. The optimum NMMW output for the photon recycler is then

$$P_\omega = \frac{\omega}{2\pi} P_o \frac{1-\mathcal{L}}{\mathcal{L}} \left(1-\sqrt{\frac{L_\omega}{\bar{G}_\omega}}\right)^2 \tag{14}$$

It is interesting to compare this with an optically pumped NMMW laser, where the absorbed infrared power for a CO_2 pump laser of the same size and loss, L, is at best P_o, the maximum infrared output power. Equation (14), shows that a photon recycler improves efficiency by a factor $(1-\mathcal{L})/\mathcal{L}$. This is due to the increased absorption possible in the hot region of the photon recycler, since the cold region restores most $(1-\mathcal{L})$ of the absorbed energy. Equation (3) shows that reducing the loss L only weakly affects output.

C. Gain and Rate Criteria

In deriving the above results for optimum photon recycler performance, a number of restrictions have been placed on the relative rates. The first is that the transit rate of molecules through the laser beam be fast compared to the excited state vibrational decay rate,

$$\frac{u}{\ell} >> \Gamma \tag{15}$$

This is the minimum restriction, since the system transit rate will be slower than u/ℓ and also must be larger than $1/\Gamma$. Infrared saturation in both hot and cold regions (see Fig. 5) demands that

$$\frac{R}{\bar{\mathcal{Z}}} \frac{\ell}{u} >> 1 \tag{16}$$

where $1/\bar{\mathcal{Z}}$ = the fraction of the total population in levels 2 and 3. Equation (16) assumes rapid velocity and rotational equilibration compared to the infrared transition rate R, so that σ_R

is a Doppler-broadened cross section. Fast rotational equilibration requires that

$$\frac{\mathcal{S}_2}{\mathcal{S}_1-\mathcal{S}_2} R \gg \gamma_R \gg R \tag{17}$$

where the left hand inequality is necessary in the cold region [see discussion following Eq. 9] to prevent rotational quenching of the NMMW inversion. NMMW saturation requires that

$$2r = 2\frac{I_\omega \sigma_\omega}{\hbar\omega} \gg \gamma_R \tag{18}$$

where σ_ω is homogeneously broadened.

In order to derive restrictions on the photon recycler geometry from Eqs. (15)-(17), the infrared intensity must be determined. For Eq. (18) to hold, the NMMW small signal gain $\bar{G}_\omega$ must be large compared to the loss, L_ω.

The infrared intensity follows directly from the condition, Eq. (2), of optimum amplifier-loss output. From Fig. 1, if the power at the entrance to the amplifier - loss combination (A-L) is defined to be P_x, then the power leaving (A-L) will be $P_x + P_o$. With P_o expended in the photon recycler as net absorption, this is self consistent. Since P_x is larger than P_o, P_x is approximately the optimum intensity of Eq. (2) multipled by the amplifier area A. Using Eqs. (2) and (3) yields

$$P_x \simeq \frac{P_o}{\sqrt{G_A L}\left(1-\sqrt{\frac{L}{G_A}}\right)} \tag{19}$$

where $\sqrt{G_A L} < 1$ is required for the uniform intensity approximation leading to Eqs. (2) and (3) to be valid (i.e., the power extracted must be smaller than the cavity power). The minimum infrared intensity using the geometry of Fig. 6 is then $P_x/h\ell$ at the exit of the hot region and at the entrance to the cold region.

A constraint on the height, h_o, in the hot region is obtained from the saturation condition Eq. (16) (ℓ drops out):

$$h_o \ll \frac{P_x \sigma_R}{\hbar\Omega \bar{\bar{z}} u_o} \tag{20}$$

where u_o is the flow speed in the hot region. It is easy to show that large small-signal absorption is automatically acheived if h_o, satisfies Eq. (20). The hot region entrance width w_o is determined from Eq. (20), which fixes $h_o u_o$, using continuity:

$$w_o = \frac{\dot{N}}{n_o u_o h_o} \tag{21}$$

where the n_o density is determined from the temperature and pressure in the hot region.

The length ℓ_o is constrained by Eq. (15) to be

$$\ell_o \ll u_o/\rho \tag{22}$$

while Eq. (17) requires

$$\ell_o h_o \gg \frac{P_x \sigma_R}{\hbar\Omega \gamma_R^o} \tag{23}$$

In the cold region conditions similar to Eqs. (20)-(23) are obtained, except $P_x \rightarrow P_x + P_o \simeq P_x$. Further, the flow velocity is determined by the nozzle expansion ratio needed to give the desired temperature drop. The left hand side of Eq. (17) restricts the density in the cold region to be comparable to that employed in ordinary optically-pumped lasers. The temperature ratio then determines the density in the hot region. An additional constraint is imposed in the cold region by demanding large NMMW saturation [Eq. (18)]. This yields

$$h_e \ell_e \ll \frac{P_o}{\hbar\Omega \gamma_R^e} \frac{\sigma_\omega}{2} \frac{1-\mathcal{L}}{\mathcal{L}} \frac{\left(1-\sqrt{\frac{L_\omega}{\bar{G}_\omega}}\right)}{\sqrt{\bar{G}_\omega L_\omega}} \tag{24}$$

Equations (24) and (23) with $o \rightarrow e$ can be used to place upper and lower limits on the NMMW small signal gain [Eq. (12)], with γ_R, h, and ℓ all evaluated in the cold reigon. It is easily shown that the maximum small signal gain is very large, while the minimum is always such that $\bar{G}_\omega \gg L_\omega$, so that the results are

consistent.

D. Nozzle

For adiabatic expansion, the chamber (hot region)-to-exit (cold region) temperature ratio and specific heat ratio $\gamma = C_p/C_v$ completely determine the nozzle area ratio, velocities and pressures as given in the proposal. The results will not be repeated here.

E. Estimates for a Favorable Molecule

We now estimate the photon recycler parameters for a realistic molecule with favorable parameters (large permanent and transition dipole moments, large ΔE, and typical values of and other rates) which combines the best possible properties of existing molecules. (Note that efficient A/O modulators are now used routinely to shift CO_2 laser frequencies into coincidence with IR molecular transitions of interest; see C. Rolland, J. Reid and B.K. Garside, Appl. Phys. Lett. 44, 380 (1984).) The results demonstrate exactly which restrictions (above) are most difficult to fulfill in practice, and are listed in Table 2, below.

TABLE 2. "Ideal Molecule" Photon Recycler Parameters.

Molecular Properties

Rotational constants: $A=10\ cm^{-1}$
$B=C=2\ cm^{-1}$
Mass: M=75 amu

Infrared transition: (J,K) = (6,5) → (5,4) (Perpendicular band)
This gives an infrared energy difference: $\Delta E \sim 100\ cm^{-1}$)
Vibrational transition dipole moment: $\mu_v = .1 \times 10^{-18}$ esu
Infrared frequency: $\Omega = 1000\ cm^{-1}$
NMMW transition: rotational (6,5) → (5,5)
Permanent dipole moment: $\mu_0 = 2.3 \times 10^{-18}$ esu
NMMW frequency: $\omega = 20\ cm^{-1}$

Rotational (ΔJ) equilibration rate: γ_R = 10MHz/torr @300°K
(Note: we assume dipole-dipole interactions for temperature scaling).

Specific heat ratio: $\gamma = C_p/C_v = 4/3$

Photon Recycler

IR amplifier-loss (see Table 1)
Hot temperature: $T_o = 150^\circ K = 105\ cm^{-1}$
Cold temperature: $T_e = 37.5^\circ K = 26\ cm^{-1}$

PR infrared absorption loss: $\mathcal{L} = 1/15$

Cold pressure = P_e = 12.5 mT @37.5°K
hot pressure = P_o = 3.3 T @150°K

Molecule flow rate: $\dot{N} = 2.7 \times 10^{22}$/sec
Mass flow rate: $\dot{M} = 3.4$g/sec
Nozzle areas: $A_t = 14\ cm^2$; $A_e = 252\ cm^2$

Optical Parameters

Infrared cross section (Doppler) $\sigma_{\mathcal{R}}^o = 2 \times 10^{-15}\ cm^2$ (hot)
$\sigma_{\mathcal{R}}^e = 4 \times 10^{-15}\ cm^2$ (cold)

Partition fraction: $1/\bar{z}_o = 1.6 \times 10^{-2}$ (hot)
$1/\bar{z}_e = 7.0 \times 10^{-4}$ (cold)

NMMW cross section $\sigma_\omega = 2.1 \times 10^{-13}\ cm^2$ (cold)
NMMW average gain per pass $\bar{\mathcal{G}}_\omega = 244/h_c\ l_c$
(see below for $h_e\ l_e$)

Infrared amplifier-loss flowing power: $P_x = 41$ W
(see text)

Optimum NMMW power output: $P_w = 1.4$ W

Nozzle Parameter Constraints

Hot region:
Width $w_o >> 1.9$ cm
laser beam areas $l_o h_o >> 10^{-2}\ cm^2$ for J equilibration
$>> 10^{-1}\ cm^2$ for K (vibrational exchange equilibration)

Cold region:
Width $w_e >> 1425$ cm
laser beam areas $l_e h_e >> 1.3\ cm^2$ (J equilibration)
$>> 13\ cm^2$ (K equilibration)
height $h_e << .4$ cm

The greatest difficulty in developing a practical photon recycler system is the need to obtain simultaneously a large ΔE

[Eq. (6)] and a reasonable partition fraction $1/\bar{Z}$ [Eq. (16)]. A large ΔE is required to reasonable temperatures for large infrared inversion in the cold region. However, a large ΔE in the rotational cooling scheme requires that both the upper and lower states of the infrared transition lie reasonably high in their manifold (high J,K), leading to low values of $1/\bar{Z}$ in the cold region. The vibrational cooling scheme presented in our original proposal provides large ΔE but requires vibrational heating in the hot region and again small $1/\bar{Z}$. The consequence of the small $1/\bar{Z}$ is high infrared saturation intensity and hence an unwieldy geometry in which the nozzle must be very wide and thin, in order to achieve saturation. This leads to an unacceptable value ofthe nozzle width, w, and height, h, in the cold region.

The large saturation intensity can be reduced in principle by working at low enough temperatures and reducing ΔE and $\bar{E}$ to increase the partition fraction. However, condensation probably is a limiting factor. A more reasonable approach may be to find a small Z system, perhaps an atom with some metastable levels which can be collisionally coupled to allowed transitions to achieve energy storage. Alternatively, the photon recycling concept can be extended and tested at other wavelengths, for example, visible to IR conversion. The flow for a given IR output power would be much smaller (10^{-3}-10^{-2}) than that of the corresponding NMMW system, and the E problem can be eliminated by using an atomic system. However, a metastable level must be employed for energy storage.

II. Energy Storage Experiments

In a photon recycler, infrared energy is stored in the hot region and extracted in the cold region. The IR laser field populates a specific ro-vibrational state (VJKM) at a given velocity and collisions transfer this energy to neighboring states (V′J′K′M′) with different velocities. It is essential to determine the range of states and velocities which are populated for the storage and extraction time scales. For this reason,

time resolved infrared-infrared double resonance spectroscopy of photon recycler candidate molecules $^{12}CH_3F$ and $^{13}CH_3F$ has been undertaken to study energy storage and transfer, particularly the relative rates of molecular energy flow into rotational vibrational and translation (velocty changing) motion. This has led to the development of a general spectrometer consisting of a stable CO_2 laser oscillator, frequency-locked to the side of its own gain profile, and a tunable infrared diode laser probe. In the experiments, the absorption of the diode laser is detected with a fast HgCdTe detector. This signal is amplified and fed to a boxcar integrator, the output of which is digitized and stored by computer. In order to generate stable, reproducible and velocity selective pump pulses for the time resolved experiments, the stable CO_2 laser oscillator output (5W) is focussed into an acoustooptic intensity modulator to obtain pulses with durations from 100 ns to c.w. For some applications, these pulses are amplified using a two meter c.w. CO_2 laser tube to obtain up to 20 W pulses. With this system it has been possible to measure collision induced J transfer rates by probing a hot band ($v_3 = 1 \rightarrow v_3 = 2$) transition and pumping the fundamental. By selecting different $v_3 = 1$ J values, both the decay of the pumped state and the transfer to neighboring J states have been studied. Also, the effective K changing rates due to vibrational exchange have been measured. Further, by using both parallel and perpendicular pump-probe polarizations, it has been possible to show that the magnetic substate distribution is not strongly altered in J-transfer. The alignment is apparently nearly preserved in such collisions.

It is of interest to study the velocity changes which accompany both J-transfer and J-preserving collisions. This is quite difficult, since the velocity changes accompanying long range interactions (dipole-dipole and Van der Waals') are apparently very small. In order to study this problem, we have developed a technique in which two pulses separated by a time delay, T, interact with the sample to create a velocity grating.

A weak tunable probe field then probes this grating. As the probe is tuned, a Ramsey resonance-like signal is obtained. It can be shown from the collisional evolution equations that to a good approximation, for a given T, the grating which is created decays exponentially at a rate which is determined by the Fourier transform of the velocity changing kernel. Hence, by measuring the probe absorption signal versus probe frequency for different time delays relative to the pump pulses, the grating decay rates for various fixed T can be determined and the kernel can be studied. For the first experiments, the probe beam was taken from the stable CO_2 oscillator and the system employed a Lamb dip configuration. Beautiful Ramsey resonance-like grating fringes were obtained (Fig. 7). Currently, we are in the process of taking data with this system and developing the complete theory of the signals. By employing a stable diode laser (He Dewar-cooled, rather than mechanical pump/refrigerator-cooled), it should be possible to extend this technique to measure with high precision, the velocity changing kernels associated with J-transfer. This will make it possible for the first time to study both the classical and diffractive contributions to molecular kernels for various processes in a single experiment. Finally, we are developing new photon techniques for collision studies using acoustooptic modulators for pulse generation. A two pulse echo is shown in Fig. 8 (large peak).

This work is forming the Ph.D. thesis research for J.M. Liang and will lead to a number of publications on new techniques for studying molecular collision dynamics.

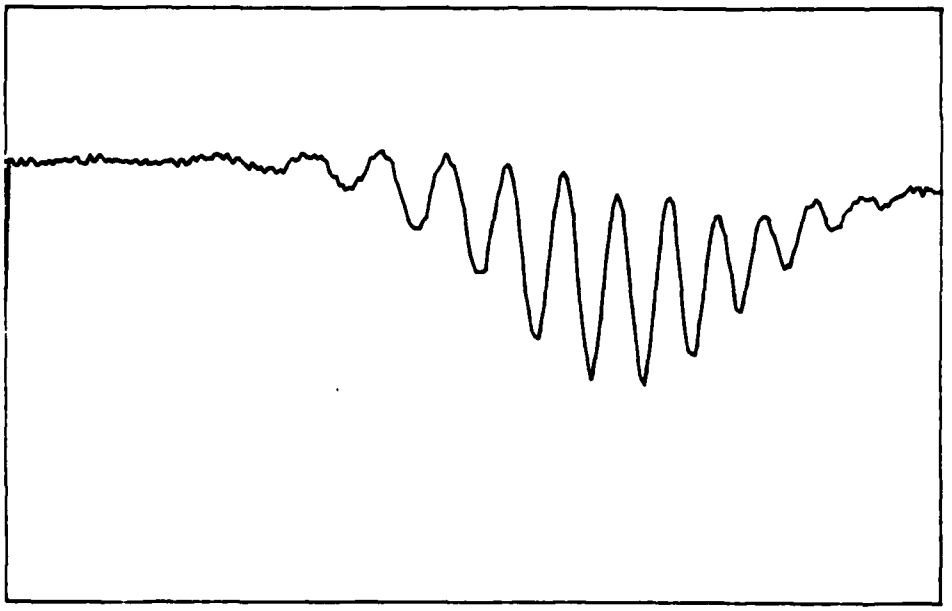

Figure 7. Probe change signal due to velocity grating.

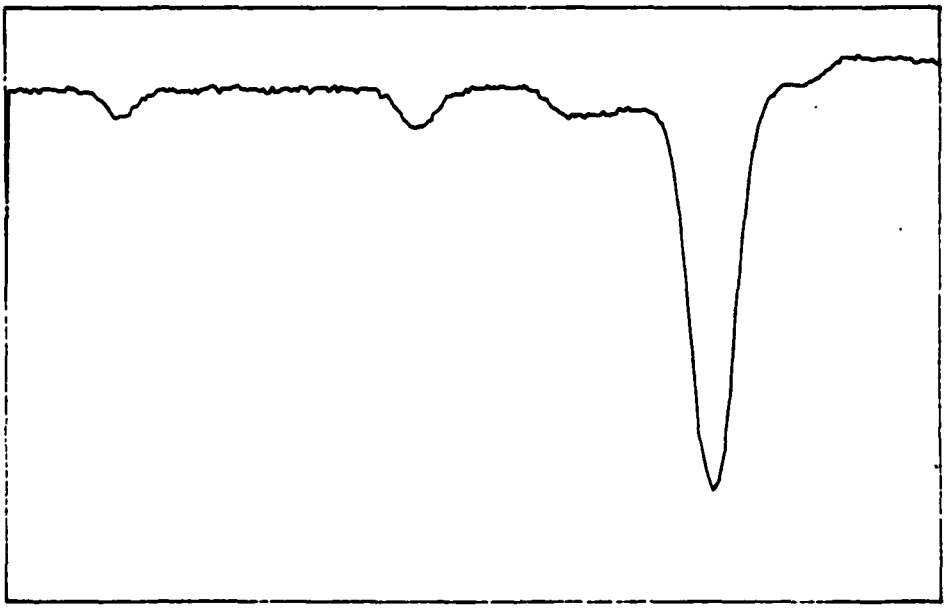

Figure 8. Two pulse photon echo.

III. PARTICIPATING PERSONNEL

Professor Michael S. Feld
Dr. Ramachandra R. Dasari (Principal Research Scientist)
Dr. John E. Thomas (Research Scientist)
Jeng-Min Liang (Graduate Student)
C. David Nabors (Undergraduate Student)

IV. PUBLICATIONS

Photon Recyclers, J.E. Thomas, R.R. Dasari and M.S. Feld, Int. Journal of Infrared and Millimeter Waves 3, 137 (1982).

Infrared-Infrared Double Resonance Studies in CH_3F J.-M. Liang, V.V. Itagi, R.R. Dasari, J.E. Thomas, and M.S. Feld, Proceedings of Third Conference on Lasers and Applications, (Kanpur, India, 1984).

Alignment Transfer for Inelastic Collisions in CH_3F, J.-M. Liang, C.D. Nabors, R.R. Dasari, J.E. Thomas and M.S. Feld, Otpics Letters, to be published.

END

FILMED

3-85

DTIC